8

The Hydrodynamic Modelling of Reefal Bays – Placing Coral Reefs at the Center of Bay Circulation

Ava Maxam and Dale Webber
University of the West Indies
Jamaica

1. Introduction

Reefal bays are a common type of bay system found along most Caribbean coasts including the Jamaican coastline. These bay systems are associated with and delimited by arching headland with sub-tending reef arms broken by a prominent channel. Traditionally, these bays are termed "semi-enclosed" as their limits are defined by the sand bar or reef partially cutting off waters behind them from open sea (Nybakken, 1997). Yet, it has been shown that circulatory patterns emanating from the lee of reef structures can persist beyond the fore-reef (Prager, 1991; Gunaratna et al., 1997). This raises the possibility of re-characterizing these systems where the reef is defined as the centre of a dynamic bay, inducing a continuous re-circulation of the inside waters beyond the traditional limit (Figure 1). In this study, hydrodynamic modelling, particle tracking and a novel gyre analysis method were used to assess the reefal bay's signature spatial and temporal patterns in circulation, with the goal of characterizing the reefal bay as unique in its function. This was carried out on the Hellshire southeast coast of Jamaica where four of seven bays are typical reefal bays.

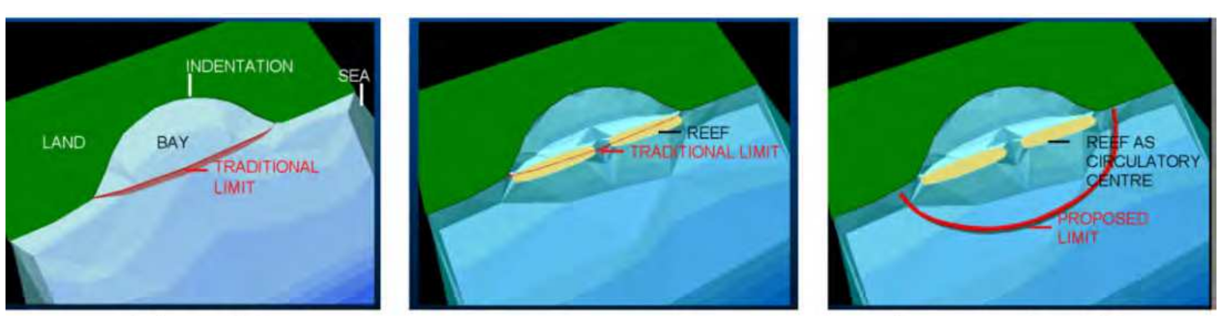

(A) open bay (B) traditional reefal bay (C) proposed reefal bay

Fig. 1. A number of hypothetical bays are presented where A represents the open bay, B the traditional definition of the reefal bay, and C the reef proposed as circulatory centre of the reefal bay system.

Reef systems often function to reduce the shoreline wave action and influence sediment dynamics. They therefore provide the ecological link between land and sea, as nurseries offering protection for marine life, as recreational sites, and as receiving sites for industrial and biological effluent. Their distinctive circulatory patterns have, however, been understudied and not fully characterized. This research aims to describe the signature circulatory patterns of the subtending reef bay system, including the effects of bathymetry, wind, tides and over-the-reef flow on this circulatory emanation. Hydrodynamic modelling, particle tracking and a novel gyre analysis method were utilized to characterize the reefal bay circulation and determine those features that make this reef-centered bay system unique.

Reefal bays carry unique patterns of circulation, however, very few reef hydrodynamic studies have focused on the particular circulation associated with fringing Caribbean reef systems. One study on a shallow, well-mixed Caribbean type back-reef lagoon in St. Croix documents that circulation was dominated by wind and over-the-reef flow (Prager, 1991). Another study on the Grand Cayman Island reefs documented that the outer reef tended to be dominated by wind-driven currents and the inner by high frequency waves. Deep water waves and tides, winds and over-the-reef flow controlled the hydrodynamic sub-system found in the lagoon (Roberts et al., 1988). At the reef crest, wave breaking and rapid energy transfers resulted in a sea level set-up which drove strong reef-normal surge currents (Roberts et al., 1992). In both the Grand Cayman and St. Croix reef systems, flow over the reef was often the dominant forcing mechanism driving lagoon circulation (Roberts, 1980; Roberts & Suhayda, 1983; Roberts et al., 1988). Whereas previous studies have contributed to Caribbean reefal hydrodynamics, their application to the reefal bay systems in particular falls short in a number of ways. The reefal bay dynamics has never been distinguished from other reef systems as a unique coastal system. It is instead often broadly categorized under the larger fringing reef system or as a fully enclosed lagoon system. Also, the contribution of reef-induced eddies to the hydrodynamic make-up is understated. Smaller-scale eddy features were not examined in these Caribbean studies. These are important features to note, whether transient or permanent in nature (Sammarco & Andrews, 1989) because of their ability to trap water, sediments, larvae and plankton around reefs. Sammarco & Andrews (1989) showed that attenuation of tidal effects within lagoons and tidal anomalies generated by the reef were responsible for creating or maintaining eddies on isolated systems. More comprehensive research is now necessary to determine the characteristic circulatory dynamics and responsible forcing functions.

2. Numerical modelling development and challenges for reef systems

The lagoons formed by coral reefs exhibit some of the most variable bathymetry of coastal oceanography and present a challenge to understanding their dynamics (Hearn, 2001). The ideal model must be able to account for all the forcing factors and conditions typical of the coral reef environment including wave and current propagation and interaction, density flows, channel exchange, reef topology and reef morphology. The modelling becomes even more complex when attempts are made to process spatial scales ranging from tens of kilometers down to sub-meter at the same time. These difficulties continue to confound localized studies of reef phenomena.

Several numerical models have been applied to lagoon hydrodynamics using one-dimensional (Smith, 1985), two-dimensional (Prager, 1991; Kraines et al., 1998) and three-dimensional models (Tartinville et al., 1997; Douillet et al., 2001). Wave breaking and overtopping remain phenomena that are difficult to describe mathematically because the physics is not completely understood (Feddersen & Trowbridge, 2005; Pequignet, 2008). The large range of combinations of reef types, shapes, tidal environments and wave climates makes all existing analyses of wave-generated flow on coral reefs limited in their applications (Gourlay & Colleter, 2005). Instrument-measured field data, however, confirm that the wave dynamics is responsible for a significant proportion of the reefal lagoon/bay hydrodynamics (Symonds et al., 1995; Hearn, 1999, 2001). As the waves break, a maximum set-up occurs near the reef edge. The maximum set-up on the reef top is proportional to the excess wave height (Hearn, 2001). The set-up creates the pressure gradient required to drive the wave-generated flow across the reef (Gourlay & Colleter, 2005). Friction coefficients are also important to consider and so these are presented as large values in recognition of the great roughness of reefs (Symonds et al., 1995). In consideration, however, of reefs with steep faces where waves break to the reef edge, wave set-up is reduced by the velocity head of the wave generated current. In this case, influence of bottom friction in the surf zone is ignored. Wave overtopping has been developed and described as two linked functions by Van der Meer (2002):- one for breaking waves applicable to more intense wave conditions (here, wave overtopping increases for an increasing breaker parameter), and the other for the maximum achieved for non-breaking waves applicable to significantly reduced wave conditions where waves no longer break over the reef.

Three-dimensional models continue to evolve in simulating wave-driven flow across a reef. An attempt is made in this chapter to simulate the three-dimensional flow associated with reefal bays by incorporating equations for wave breaking and overtopping at the reef into a finite element-based model for stratified flow.

3. Reefal bay sites

Southeast of Jamaica, a 15 km stretch of coastline, the Hellshire east sector (Figure 2), consists of seven bays - four of which are reefal. Three bays were compared for their circulatory signatures – Wreck Bay, Engine Head Bay and Sand Hills Bay. Two of the three, Wreck Bay and Sand Hills Bay, have prominent reef parabola stretching between headlands with a central, narrow channel breaking the reef continuum. Wreck Bay, with its narrower channel, is more enclosed than Sand Hills Bay. Associated reefs are emergent and exposed, more so at low tide. Both reefal bays are separated along the coastline by Engine Head Bay, an open bay with no development of reef arms. Engine Head Bay was therefore considered as a control given it is non-reefal and its position exposes it to the same conditions as the two reefal bays.

A diurnal variation in the wind records is typical of the southeast coast of Jamaica (Hendry, 1983) due to the influence of the sea-land regime. The tidal range is microtidal ranging from 0.3 - 0.5 m with an annual mean of 0.23 m (Hendry, 1983) and demonstrating a mixed tidal regime. Tidally generated currents are therefore small in amplitude compared to wind-driven currents. The wave climate of the southeast coast is influenced mainly by trade wind-generated waves that approach Jamaica from the northeast. Offshore waves impact the shelf edge off Hellshire from a predominantly east-south-easterly direction after undergoing southeast coast refraction. Swell waves approach the coast at a typical period range of 6-9 seconds, but these are soon affected by complex bathymetry. Wave decay occurs when the land-breeze emanates along the coast. The shelf along which these bays fringe are made up of basement rock composed of Pliestocene limestone eroded during low sea levels in the Pliestocene epoch. As a result, bathymetric highs are now shoals, banks, reefs and cays, and on the inshore, karst limestone relief facilitates freshwater sub-marine seeps into the bays (Goodbody et al., 1989).

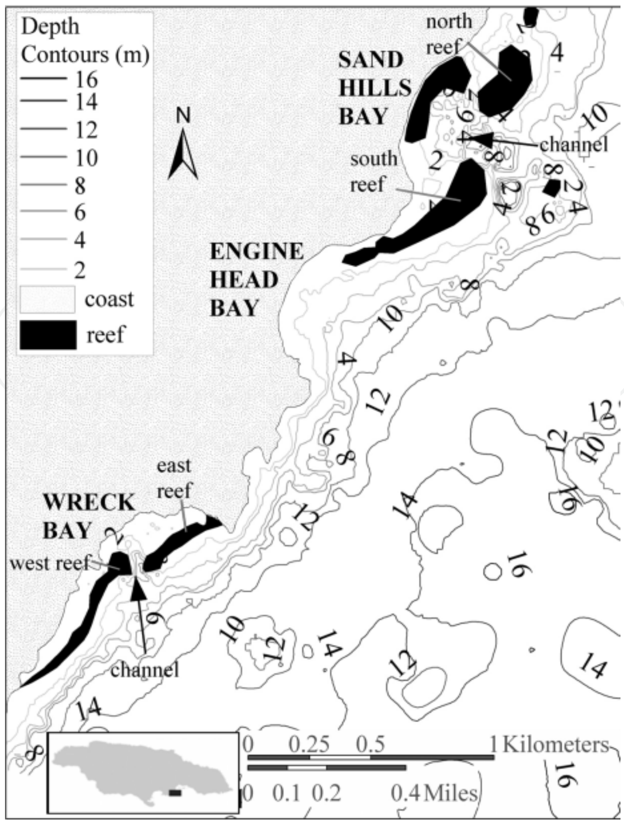

Fig. 2. Map showing the study site of three bays located on the Hellshire South East Coast of Jamaica. Wreck Bay and Sand Hills Bay are the two reefal bays under investigation, along with the open bay Engine Head Bay located between the other two.

Environmental stress studies conducted inshore and offshore these bays used plankton population size and species composition as indicators. Lowest values in biomass, primary production and density were recorded in the southernmost bays. These bays were therefore considered generally removed from the effects of the highly productive Kingston Harbour and Great Salt Pond waters to the north, with the exception of during flood occasions when elevated levels were recorded in the southernmost bay, Wreck Bay. The authors suggested the possibility of long retention times due to localized circulation (White, 1982; Webber, 1990). These results were of great interest given the implications presented for the protective role played by reefal bays as nurseries for the early aquatic stages of marine and terrestrial species; for the significance of its distance down-shore from the main harbor not inhibiting its eutrophication; and for sediment transport and exchange along the shoreline. In fact, physicochemical variables were also robust in characterizing the persistence of bay waters beyond the reef (Maxam & Webber, 2009). This indicated the need for appropriate numerical simulations to adequately describe the circulatory patterns in these bays - the findings of which are presented in this chapter.

4. Methods for Simulating the reefal bay system

Oceanographic and meteorological data were collected for the Hellshire coast and served as inputs into the hydrodynamic model. Field data were also used for model verification after executing model simulations under various meteorological conditions. This was followed by an analysis of bay contraction and expansion due to circulation induced by the presence of the subtending reef, and ultimately the development of particular circulatory signatures defining the reefal bay.

4.1 Oceanographic and meteorological data collection

Bathymetric depth points were digitized from Admiralty bathymetric charts for the Hellshire coastline area and the entire South-East Shelf. For the finer-scale bathymetry required of the reef and bay areas, water depth (± 0.1 m) was measured to supplement the Admiralty data using an echo-sounder with Trimble Garmin GPS and post processed to account for tidal elevation differences from mean sea level. Wind speed (± 0.1 m s^{-1}) and wind direction (± 0.1°) data were collected from the nearby Normal Manley International Airport weather center as continuous two-minute averages over the entire sampling period (1999 to 2003). Long-term current measurements for speed (± 0.10 cm s^{-1}) and direction (± 0.1°) were recorded continuously by Inter-Ocean S4 current meters at four sites inside (Table 1) and outside of Wreck Bay.

	Mooring Location	Depth (m)	Deployment Dates	Duration (wks)	0n / every
1	Channel	4.0	24 May – 13 Jun 2000	3	5 min / 1 hr
2	Channel	4.0	11 Jul – 03 Sep 2000	7	5 min / 1 hr
3	Channel	4.0	20 Dec 2002 - 10 Jan 2003	3	1 min / 10 min
4	Channel	4.0	14 Mar – 28 Mar 2003	1	1 min / 10 min
5	West Back-reef	2.0	11 Jul – 03 Sep 2000	7	5 min / 1 hr
6	East Back-reef	0.7	20 Jul – 01 Sep 2000	1	5 min / 1 hr

Table 1. Deployment specifications for long-term field current data collection in Wreck Bay. Hydrodynamic model outputs were compared with these measurements for verification.

Hourly tidal amplitudes (± 1 mm) were calculated using Foreman's Tidal Analysis (Foreman, 1977) and Prediction Program, incorporating mean sea-level and tidal amplitude data over a 40-year period from Port Royal, a nearby tide station. Hourly incident wave height values (± 1 cm) used in the over-the-reef flow calculations were taken from Refraction-Diffraction (REFDIF) wave models (Kirby & Dalrymple, 1991) of the shoreline (Burgess et al., 2005). The deepwater wave climate obtained from JONSWAP (Hasselmann et al., 1973) analysis was used to run the REFDIF models in order to carry the deepwater waves from the continental shelf to the shoreline. Near-shore conditions were simulated at 50% occurrence (average conditions) and used as input into the hydrodynamic model.

4.2 Hydrodynamic modelling

A hydrodynamic model, RMA-10, was utilized to simulate the depth-averaged velocity field of the fore-reef and back-reef along with the shoreline flow under wind and tidal conditions typical of the Jamaican south-east coastal area. RMA-10 is a three-dimensional finite element model for simulation of stratified flow in bays and streams (King, 2005). The primary features of RMA-10 are the solution of the Navier-Stokes equations in three-dimensions; the use of the shallow-water and hydrostatic assumptions; coupling of advection and diffusion of temperature, salinity and sediment to the hydrodynamics; the inclusion of turbulence in Reynolds stress form; horizontal components of the non-linear terms; and vertical turbulence quantities are estimated by either a quadratic parameterisation of turbulent exchange or a Mellor-Yamada Level 2 turbulence sub-model (Mellor & Yamada, 1982). Computations in the model are based on the Reynolds form of the Navier-Stokes equations for turbulent flows and employ an iterative process that solves simultaneous equations for conservation of mass and momentum. RMA-10 requires the input of nodal x, y and z data depicting sea floor bathymetry, parameters for roughness and eddy viscosity, and boundary conditions of flow discharge. The iterative process computes nodal values of water surface elevation, flow, depth and layered horizontal velocity components or vertically averaged velocity components if this option is used.

Two-dimensional depth-averaged approximations were used for the Hellshire bays' simulations. Depth-averaged results are appropriate given the shallowness of the reefal bay and the knowledge that this usually presents a well-mixed system. Boundary conditions were entered into RMA-10 using a list of nodes defined as flow continuity checks simulating flow over the reefs and also used to specify initial values of salinity concentration (36.0 ppt), temperature (28.0 °C) and suspended sediment concentration (2.0 μgL^{-1}) conditions along the model east and west open boundaries. Boundary conditions were also read from a wind velocity and direction file derived from wind data. This was input as hourly averaged wind velocity and direction and allowed the model to read dynamic wind conditions useful in examining the influence of a diurnal wind regime. Boundaries were also subject to a tidal-graph of hourly tidal elevation data for interpolation.

Reef parabola were represented by continuity lines where hydrograph data of dynamic flow over the reef were interpolated. Flow over the reef was calculated as hourly-averaged values using the wave run-up and overtopping Van der Meer equations (Van der Meer, 2002) as a base. Wave overtopping is the average discharge per linear meter of width, q, and is calculated in relation to the height of the reef crest line. The final flow value Q used in the hydrograph file is given as the length of the reef parabola long axis multiplied by the average discharge q. For breaking waves ($\gamma_b \xi_0 \leq 2$), wave overtopping increases for increasing breaker parameter ξ_0. Assumptions are made of a fully developed wave at the reef crest and so the incident wave height is used. Determination of correct wave period for heavy wave-breaking on a shallow fore-shore is neglected here as this requires complex wave transformation Boussinesq models (Nwogu et al., 2008) and lies beyond the objectives of this study. Instead, an average value for the wave period is used. Other influences are included in the general formula such as roughness on the reef slope and the reef slope itself (considered here to be equal to or steeper than 1:8 close to the reef crest). The wave overtopping formula is given as exponential functions with the general form:

$$q = a \cdot \exp(b.R_c) \quad (1)$$

The coefficients a and b are still functions of the wave height, slope angle, breaker parameter and the influence factors of reef roughness and slope; R_c being the free crest height above still water line. Wave heights used varied around the predicted value of 0.48 m but were not simulated for extreme events (<1-year event occurrence). A set of turbulent exchange, turbulent diffusion and Chezy coefficients was applied at all nodes. The turbulent exchange coefficient associated with the x and y direction shear of the x and y direction flow was set as -5.4 Pa s. The turbulent exchange coefficient of the z direction shear of the x and y direction flow was set at 0.44 Pa s. The turbulent diffusion coefficient associated with the x and y directions were set at 2.11 $m^2 s^{-1}$ and that associated with the z direction set at 0.21 $m^2 s^{-1}$. The Chezy coefficient of 0.029 $m^{0.5} s^{-1}$ was used for all nodes except at the shoreline where it was reduced to 0.0015.

Particular conditions at the Hellshire coastline led to adding a third variable, Y, to account for the diurnal effect of the wind regime. It was found that emanation of the land-breeze significantly reduced wave heights and caused more variation in the flow over the reef than predicted by the Van de Meer calculations. This variable Y is a function of the southward wind flow and leads to a large reduction in the q value once the land-breeze emanates. At a maximum the final overtopping formula becomes:

$$\frac{q}{\sqrt{gH_{m0}^3}} = 0.2 \cdot \exp(Y) \cdot \exp\left[-2.3\,\frac{R_c}{H_{m0}}\,\frac{1}{(\gamma_f)(\gamma_b)}\right] \qquad (2)$$

where:

q	=	average wave overtopping discharge	($m^3 s^{-1} m^{-1}$)
g	=	acceleration due to gravity	($m s^{-2}$)
H_{m0}	=	significant wave height	(m)
R_c	=	free crest height above still water line	(m)
Y	=	wind y component	
γ_f	=	influence factor for roughness	
γ_b	=	influence factor for slope	

Comparisons between RMA Model results and field-collected current measurements were tested for significance using the t-test.

The model mesh was built using assemblages of two-dimensional triangular and quadrilateral elements. The software RAMGEN (King, 2003), a graphics based pre-processor for RMA-10, was used to form the grid and create the interface file that the RMA software utilized. The regional mesh covered the entire south-east coastal shelf including Kingston Harbour to the north, and had two open boundaries - one at the east side and the other south-west. Courser elements (>1 km^2) were created for the offshore shelf areas. Elements were more refined (<100 m^2) closer to the shoreline or in areas where there were expectations of large changes.

Individual particles were tracked based on the velocity distribution used by the RMATRK software (King, 2005). This application is designed to track particles released into a surface water system that have been simulated with the RMA-10 model. It transports discrete objects through a surface water system defined by the RMA-10 finite element grid. Time steps were set up so that track increments were drawn for every six minutes in a one-hour or three-hour time block.

4.3 Gyre analysis

The horizontal expansion and contraction of gyres were measured to quantify the extent of bay fluctuation. Tracks produced by the RMATRK model were of three categories:

- Hourly plotted tracks: where new particles were introduced in the same positions at the beginning of each hour for as long as the duration of one and a half tidal cycles,
- Three-hourly tracks: where new particles were introduced in the same positions at the beginning of each three-hour time block for as long as the duration of one and a half tidal cycles, and

- Indefinite tracks: where one set of particles was tracked for as long as they remained in the reefal bay system - their paths plotted for every three hours they remained.

Hourly plotted tracks were used to predict the duration of a reef gyre. Three-hourly tracks were plotted to capture the full horizontal extent of the circulation.

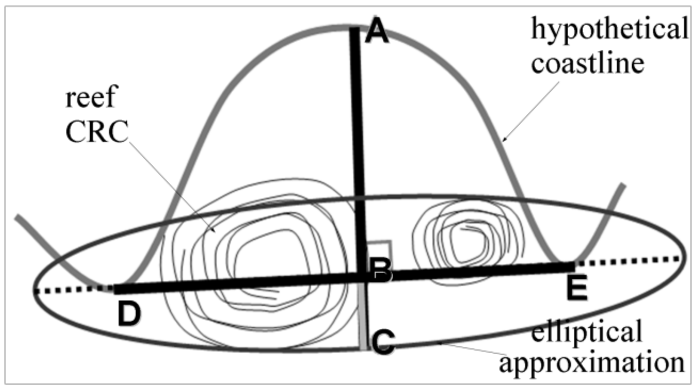

Fig. 3. Diagram of the reefal bay dimensions used in calculating the circulatory extent of the bay. The extent (BC) is calculated as a fraction of the AC distance normal to a line (DE) joining the land projections. AC is derived from an elliptical approximation of the outer, seaward curve of the looping currents.

Extents were measured from these plots as a proportion of the linear distance, from the shore to the elliptical arc, normal to a straight line joining the land projections at the ends of the bay indentation (Figure 3). The ellipse best approximates the seaward edge of the gyre. The elliptical major axis is always equal to or greater than the length of the straight line joining the land projections. Therefore, the reef circulation lateral extension, L_c, is given as the percentage:

$$L_c = \frac{BC}{AB} \times 100 \tag{3}$$

Indefinite tracks allowed predictions of the retention ability of gyres. The number of particles remaining around the reef was counted after each 3-hr track run.

5. Results

5.1 General current flow description based on field measurements

Results from fixed S4 current measurements in Wreck Bay (Figure 4) showed water flowing through the channel generally exited in a south-south-eastward direction, with a deflection southwards when current speeds were high.

Mean speed values for channel currents peaked at 22 cm s^{-1}, and flow directions were southward from 173° to 181°. On the western arm speeds averaged 28 cm s^{-1} with a mean flow direction of 102°, and on the eastern arm mean speed was 22 cm s^{-1} with a flow direction of 290°. Flow persisted southwards out through the channel from the back-reef currents continuously, except during very rare occasions of in-flow at mid-depth when velocities were at their lowest (mean of 2.9 cm s^{-1}). Channel currents in Wreck Bay were greatly influenced by the back-reef feeder currents, more than the direct influence of wind and tides. Correlations of channel and back reef flow components showed that the western arm current magnitude was almost five times more strongly correlated (cross correlation r =

0.62) than the eastern arm currents (cross correlation r = 0.18) with channel currents. The west reef feeder currents therefore contributed much more to channel flow than the east reef. Multiple regression values showed that the back-reef currents combined accounted for 47% of the variability in the channel currents, compared to wind and tides accounting for 29%.

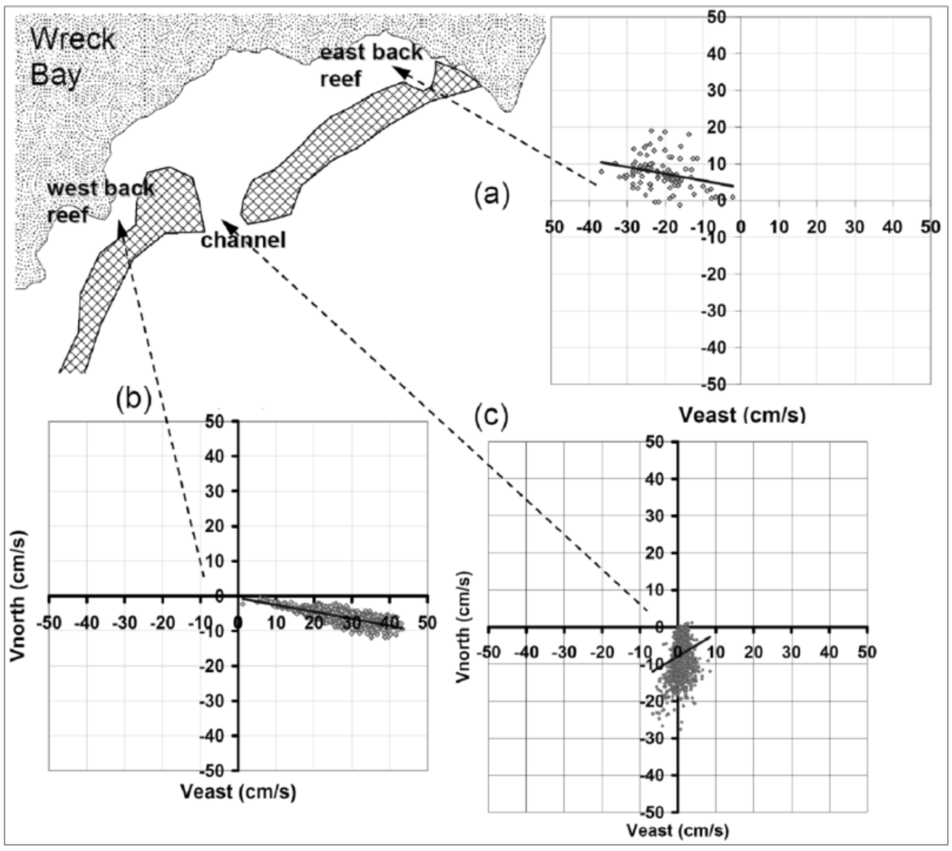

Fig. 4. Current component plots are shown for the east back-reef (a), the west back-reef (b) and channel (c) of Wreck Bay, collected from long-term deployment of S4 current meters moored at all three sites at the same time. This field data compared favorably with RMA model results.

Accountability by winds and tides of the overall variability in the current magnitude decreased from highs of 55-56% for the spring and winter data to 29% for the summer currents. During this summer period the lowest recorded mean channel current speed (7.7 cm s^{-1}) was observed as well as an equality of the relative contributions of tides and winds to the overall variability.

5.2 RMA model simulations

5.2.1 Current flow

Velocity results from S4 current meters compared well with RMA model results (depth averaged) for the dominant north (Y) component of the channel site at Wreck Bay (Figure 5), giving no significance for difference by t-test. For the month of August (2000) , S4 north component readings averaged -7.8 cm s^{-1} while the RMA model averaged slightly lower at -8.2 cm s^{-1} (Table 2). The north component was used to represent the channel flow given its high cross-correlation value of -0.99 with the channel flow magnitude.

Depth-averaged velocity results from hydrodynamic modelling showed that currents circulated the reef arms constantly. This circling of the reef was strongest during the combined condition of a rising tide with prevalent sea-breeze (Figure 6). This particular condition generated some of the strongest currents on the west reef of Wreck Bay (the 28 to 32 cm s^{-1} category) and the corresponding south reef of Sand Hills Bay. Back reef current highs by the model, however, were less than measured in the field. Field-measured monthly average for the Wreck Bay east back reef current magnitude was 22 cm s^{-1} and agrees with model averages, however, the variation in flow is not replicated and spikes in back reef speeds (up to 38 cm s^{-1}) not captured. In Sand Hills Bay, model currents strongly circulated the south reef at up to 28 cm s^{-1} on the southern curve of the gyre. Engine Head Bay showed no formation of looping currents. The combination of a prevalent sea-breeze with falling tide strengthened the east reef circulation in Wreck Bay (Figure 7). Horizontal current fields depicted velocities of up to 32 cm s^{-1} in this gyre, the fastest speeds occurring on the western side of the gyre. For Sand Hills Bay, the north reef gyre was pronounced with a central inner gyre showing closed circulation. Horizontal current fields depicted velocities of the 18 to 20 cm s^{-1} category around the north reef. Engine Head Bay again showed no formation of horizontal circulatory currents.

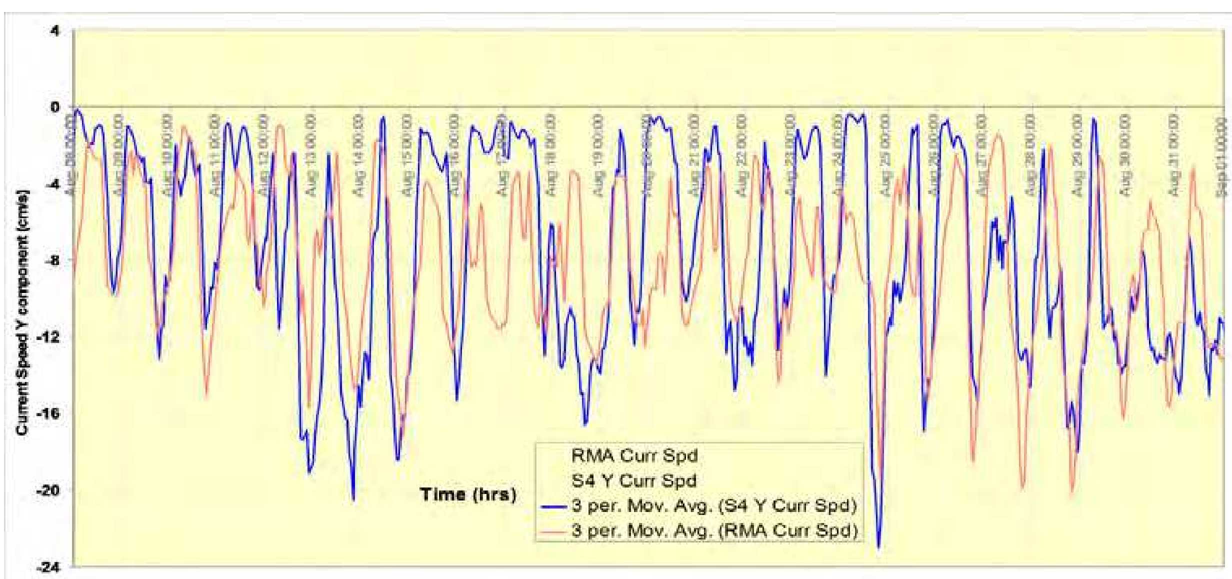

Fig. 5. RMA model and S4 field north component current data comparisons for the Wreck Bay Channel area. A t-test reported no significance for difference when both current data sets were input as independent samples ($t = 1.46$; $p = 0.15$).

	Y-COMP VELOCITY RESULTS (cm s^{-1})	
	RMA Model Data	S4 Field Data
Average:	-8.2	-7.8
Maximum:	-0.7	0.3
Minimum:	-24.5	-24.7
Range:	23.8	25.0

Table 2. RMA model and S4 field north component current data statistics and comparisons for Wreck Bay Channel.

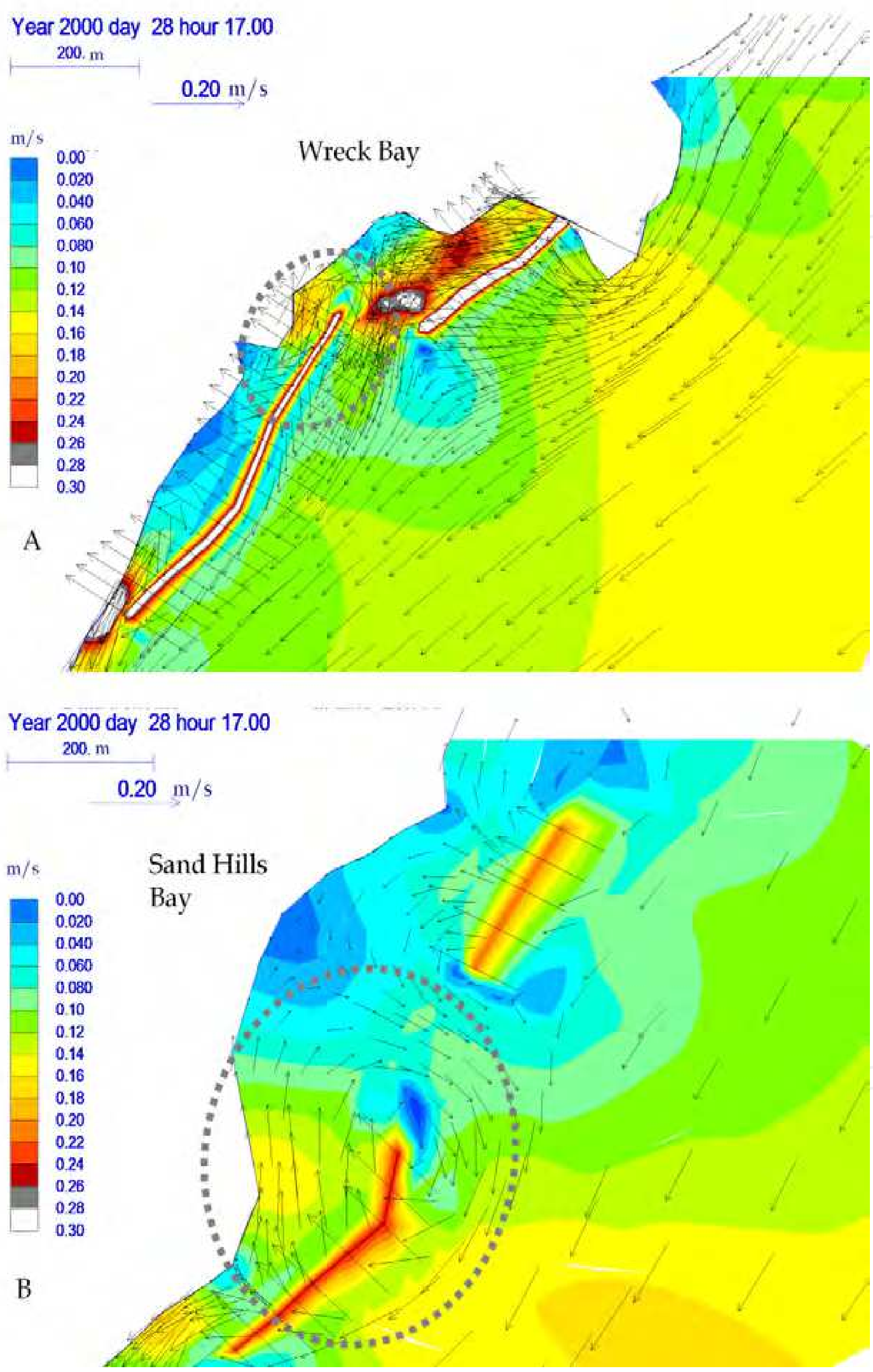

Fig. 6. Depth-averaged current field maps for (a) Wreck Bay and (b) Sand Hills Bay during a dominant rising tide combined with sea-breeze regime. Current vectors depict well-formed, closed looping circulation on the down-shore reef arm (circled), causing both bays to be expanded beyond the reef.

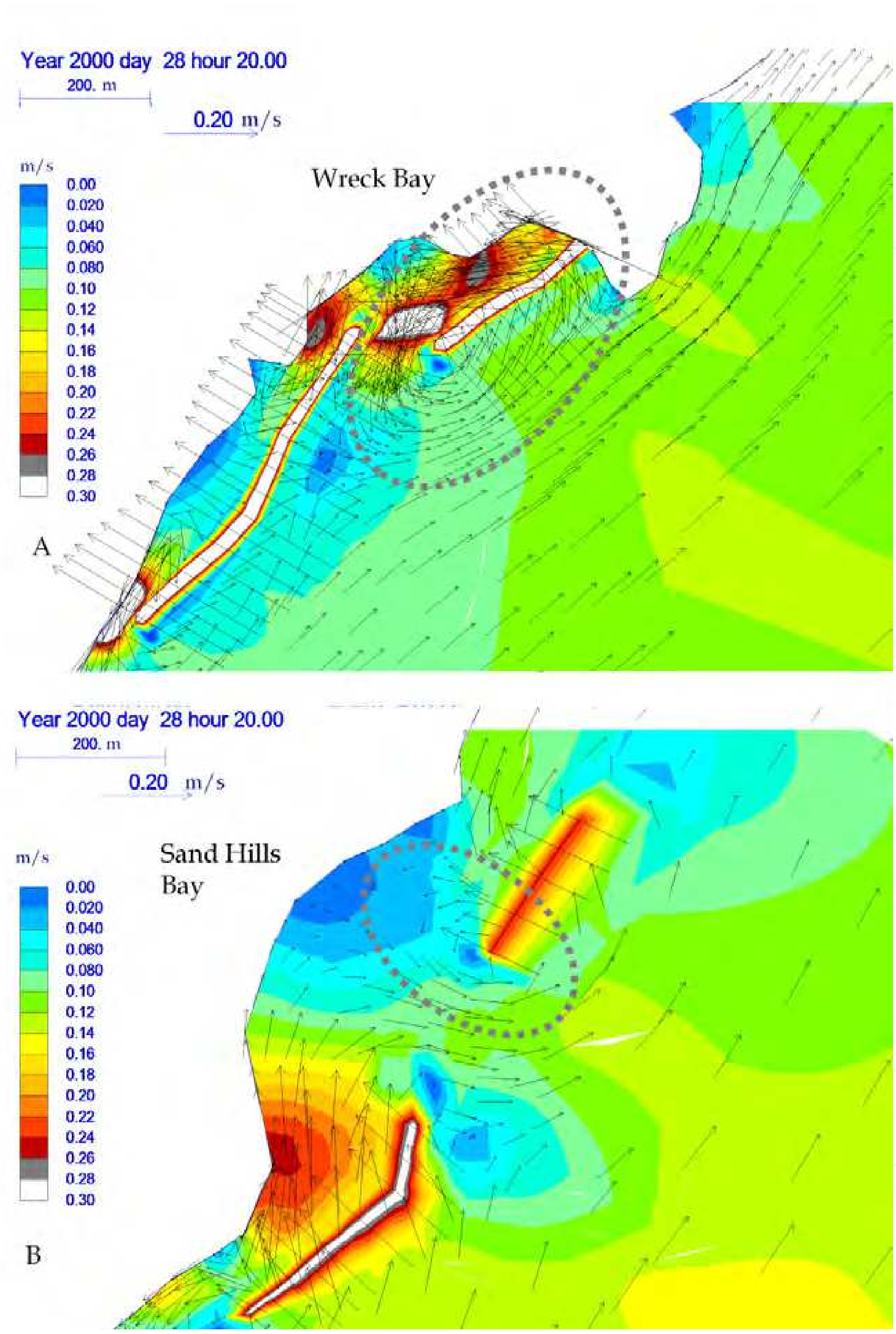

Fig. 7. Depth-averaged current field maps for (a) Wreck Bay and (b) Sand Hills Bay during a dominant falling tide combined with sea-breeze regime. Current vectors depict well-formed, closed looping circulation on the up-shore reef arm (circled), causing both bays to be expanded beyond the reef.

5.2.2 Particle tracking and retention

Under only the rising tide regime, 19 % particles remained in Sand Hills Bay after 9 hrs. The rising tide combined with land-breeze regime increased the remaining particles to 22 % after 9 hrs. When the sea-breeze dominated, however, combined with the rising tide the retention dropped to 2 % in 9 hrs. Therefore particles were likely to remain trapped in Sand Hills Bay the longest when introduced at the beginning of the rising tide cycle during a land-breeze regime and were likely to be flushed out the quickest if introduced during the sea-breeze with mid-falling tide.

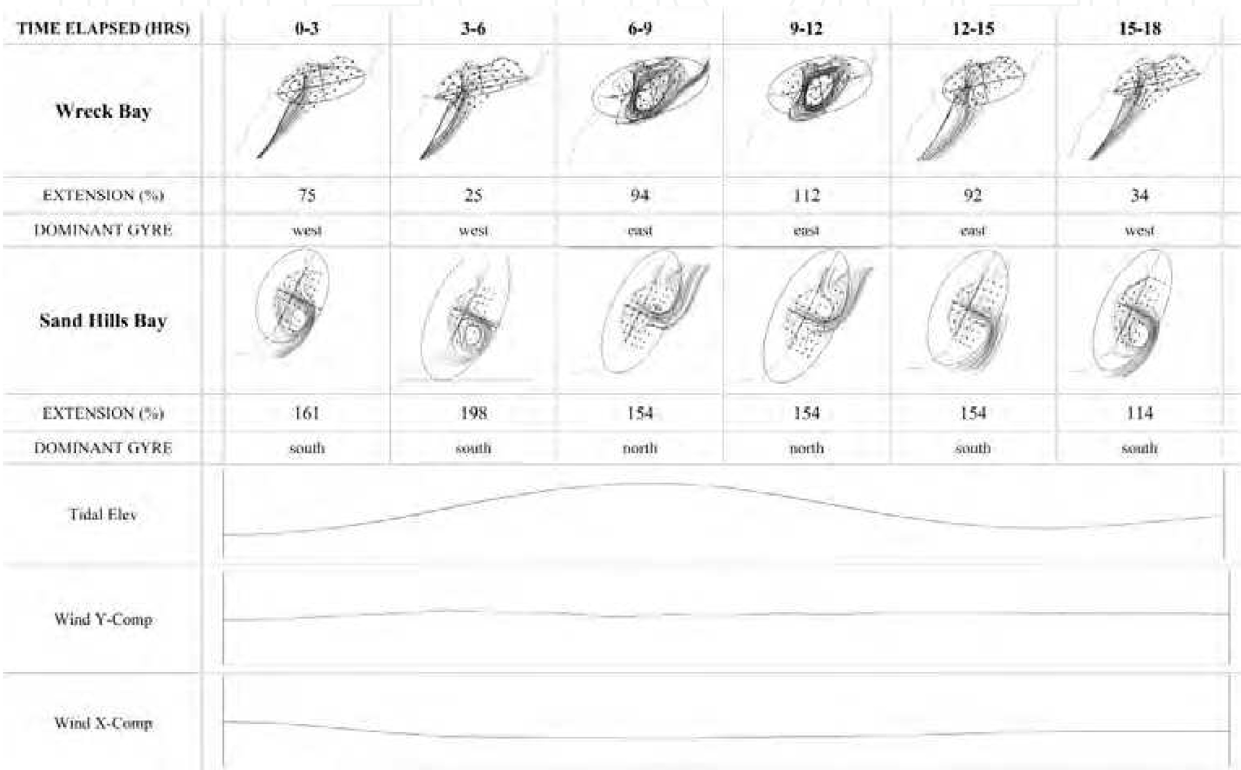

Fig. 8. Reef gyre extension measurements for Wreck Bay and Sand Hills Bay during 18 hrs (1.5 tidal cycles) of highest Y-component current speeds recorded in Wreck Bay. Tracks are displayed as time progresses in 3-hr increments for new particles introduced into the bay every three hours. Gyres undergo expansion and contraction but are always present.

Under only the falling tide regime, 36 % particles remained in Wreck Bay after 6 hrs. The falling tide combined with land-breeze or sea-breeze regime decreased the remaining particles to 6 % and 10 % respectively after 6 hrs. Therefore particles were likely to remain trapped in Wreck Bay the longest if introduced at the beginning of the falling tide cycle and were likely to be flushed out the quickest if introduced at the beginning of the rising tide.

5.3 Gyre extension assessment

Gyres expanded and contracted around reefs as the forcing conditions changed (Figure 8). As the gyre on one reef arm strengthened the other weakened. Wreck Bay had its largest extension (L_c = 112 %) during the falling tide phase and when the sea-breeze emanated. The largest extensions were produced by the east reef circulation and coincided with the greatest current component speeds flowing out of the channel. This channel current formed the western edge of the east gyre. When the west reef circulation emanated, gyre extensions were smaller and did not exceed 75 %. West reef gyres were most developed at low-to-rising tide during land-breeze emanation and coincided with the lowest current component speeds recorded in the channel at that time. The longest duration of this closed western gyre was observed during 15 hrs of some of the smallest tidal changes recorded.

Sand Hills Bay had its largest extension at 198 % during the combination of a rising tide and when the sea-breeze emanated. This was due to the south reef gyre that also tended to be more closed than the north reef's. The north reef gyre was most developed at the rising-to-high tide (also when the sea-breeze emanated) and had its largest extension at 154 %. In the absence of large tidal changes and developed wind regimes, the south gyre dominated the extension.

6. Discussion

6.1 Circum-reef circulation defining the reefal bay

Hydrodynamic modelling showed that circulation around the Wreck Bay and Sand Hills Bay reef parabola continuously looped the reef as circum-reef circulation (CRC). The CRC was considered "closed" when fore-reef currents fed water back into the back-reef and "open" when main fore-reef flow continued along-shore (Figure 9). Channel surge currents were responsible for the propagation of inner bay waters seawards, and encouraged open CRC. Tracking models revealed the longevity and spatial spread of this flow, simulating the patterns first observed in these bays by field drogues and fixed measurements that depicted continuous current flow around reef arms at surface and depth (Maxam & Webber, 2010). The presence of the reef induced this persistence and localized the (CRC). The lack of reefs in Engine head bay supported this premise as gyre formation and localization was not evident in the non-reefal bay. This was confirmation that open bays did not facilitate recycling of their inside waters from the outside as reefal bays do. In the absence of prominent reef arms, the CRC cannot exist.

6.2 Reef arm crc dominance and cycling

Simulations of new particles introduced into the bay on an hourly basis revealed that under particular tide and wind regimes, one reef's circulation was strengthened while the other abated in the same bay (Figures 10, 11). This simulated the dynamics that prevented field drogues from entering the weaker reef gyre while trapped in the dominant one (Maxam & Webber, 2010). The dominant gyre was responsible for the greatest extensions of the bay system, and so the presence of two prominent reef arms resulted in regular switching of dominance.

Full development of both reef arm gyres occurred in one tidal cycle. The reef gyre down-stream the main long-shore flow appeared strengthened on the rising tide while the adjacent reef up-shore was strengthened by the falling tide. It is important to note that these simulations accurately portray the importance of the tidal influence in a micro-tidal environment where it was otherwise expected to be overwhelmed by wind- and wave-induced stresses. In the absence of large tidal fluctuations, as during a neap tide, the up-shore gyre was too weak to be developed and the down-shore gyre dominated. Up-shore reef arms were more reliant on tidal changes to effect gyre formation than down-shore reefs. The sea-breeze aided in strengthening both gyres during simulation, agreeing with long-term field data that showed this correlation (Maxam & Webber, 2010). This wind regime

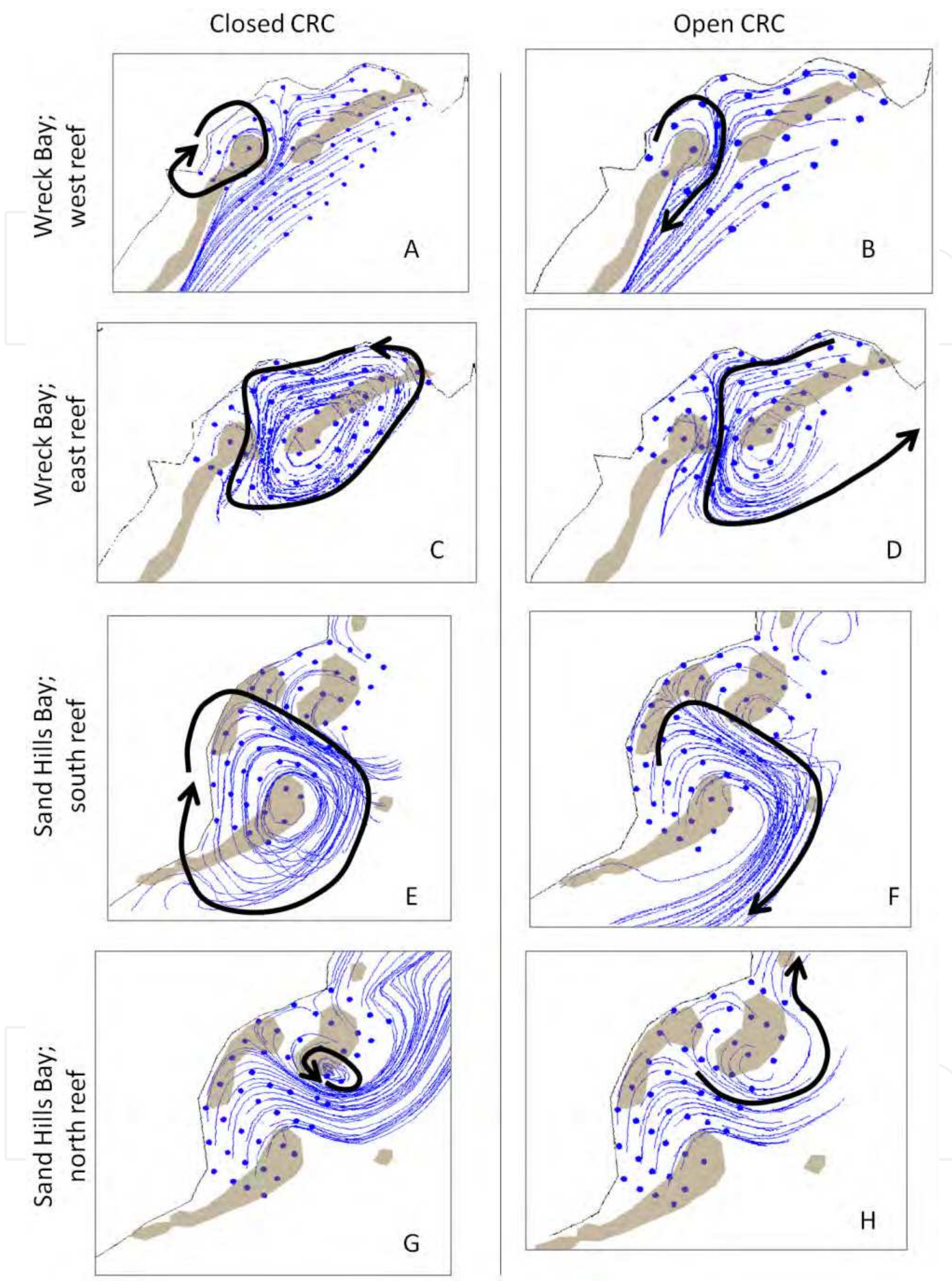

Fig. 9. Diagrams depicting closed and open circum-reef circulation (CRC) simulated from RMATRK discrete particle tracking modelling. The closed CRC displaying recirculation were evident for Wreck Bay west reef (A) and east reef (B) arms, as well as Sand Hills Bay south reef (C) and north reef (D) arms particularly during wind calms. Open CRC is also displayed in Wreck Bay west reef (E) and east reef (F) arms, and again around Sand Hills Bay south reef (G) and north reef (H) arms particularly during increased channel flow.

induced more flow over the reef due to increased heights of waves impinging on the reef and at higher frequencies (Roberts et al., 1992). Breaking would occur and the rapid energy transferred caused an increase in water level, driving strong back-reef surge currents and increasing current speeds in the northern part of the gyre. These surges, however, reduced the retention times of these gyres.

This cycle of emanation and contraction is characteristic of the reefal bay system, giving the reefal bay a spatial pulse that is dependent on prevailing wind and tidal regimes. The reefal bay does not have a static bay area but instead will be at a minimum when the CRC is most contracted and at a maximum when the CRC is most extended. At its minimal spatial extent, the horizontal area of the hydrodynamic reefal bay is dependent on the size of the reef. The larger reef in Wreck Bay, the east reef arm, gave the lager dominant gyre resulting in the greater seaward extensions of the bay. The same was observed in Sand Hills Bay where the south reef was the larger reef and therefore gave the greater extensions (Figure 12).

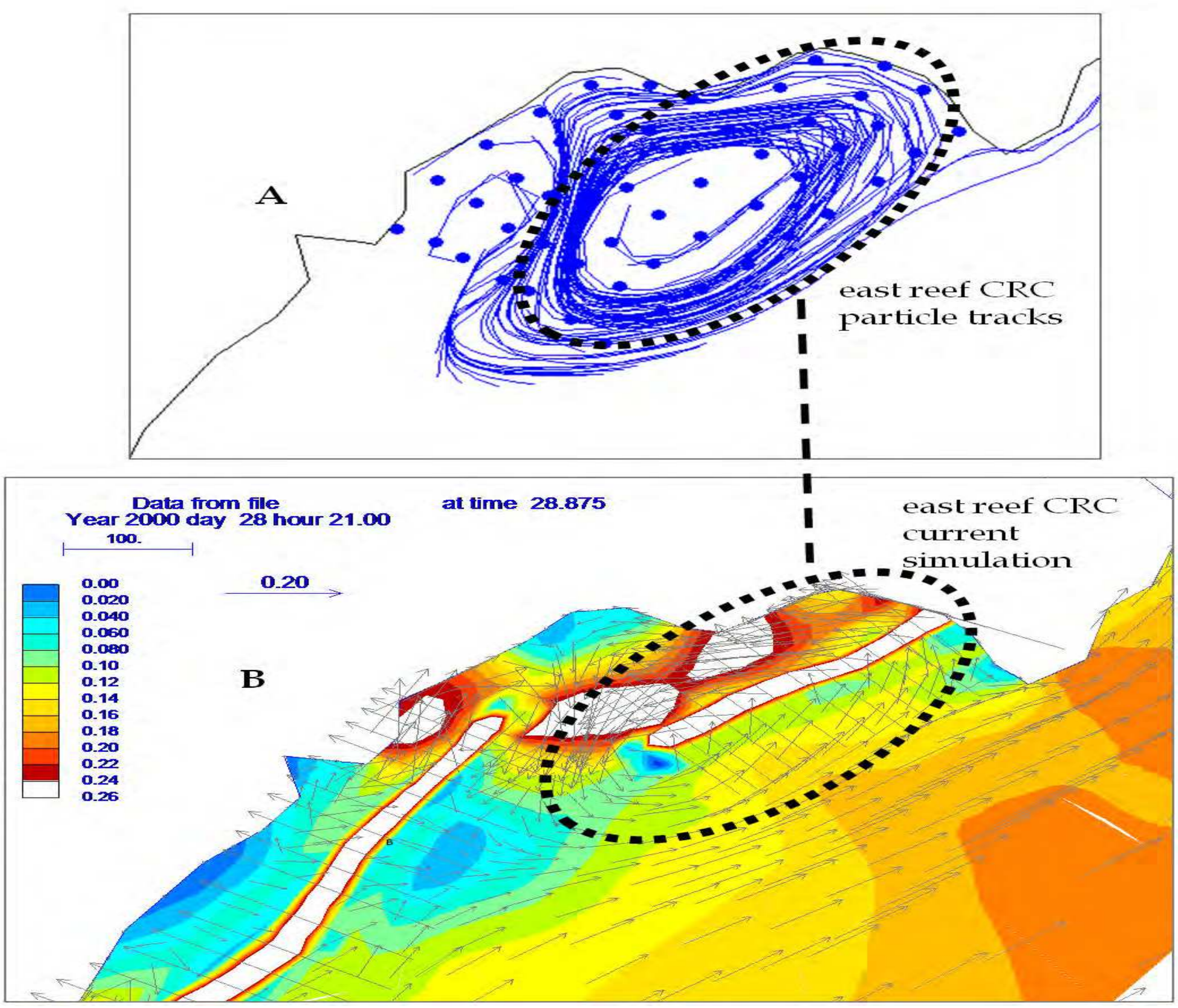

Fig. 10. Dominant east reef CRC in Wreck Bay due to large falling tide range is displayed in A and B as circled area in model particle tracks (A) and model vectors (B). CRC formation on the opposing reef arm is weakened during dominance of the other.

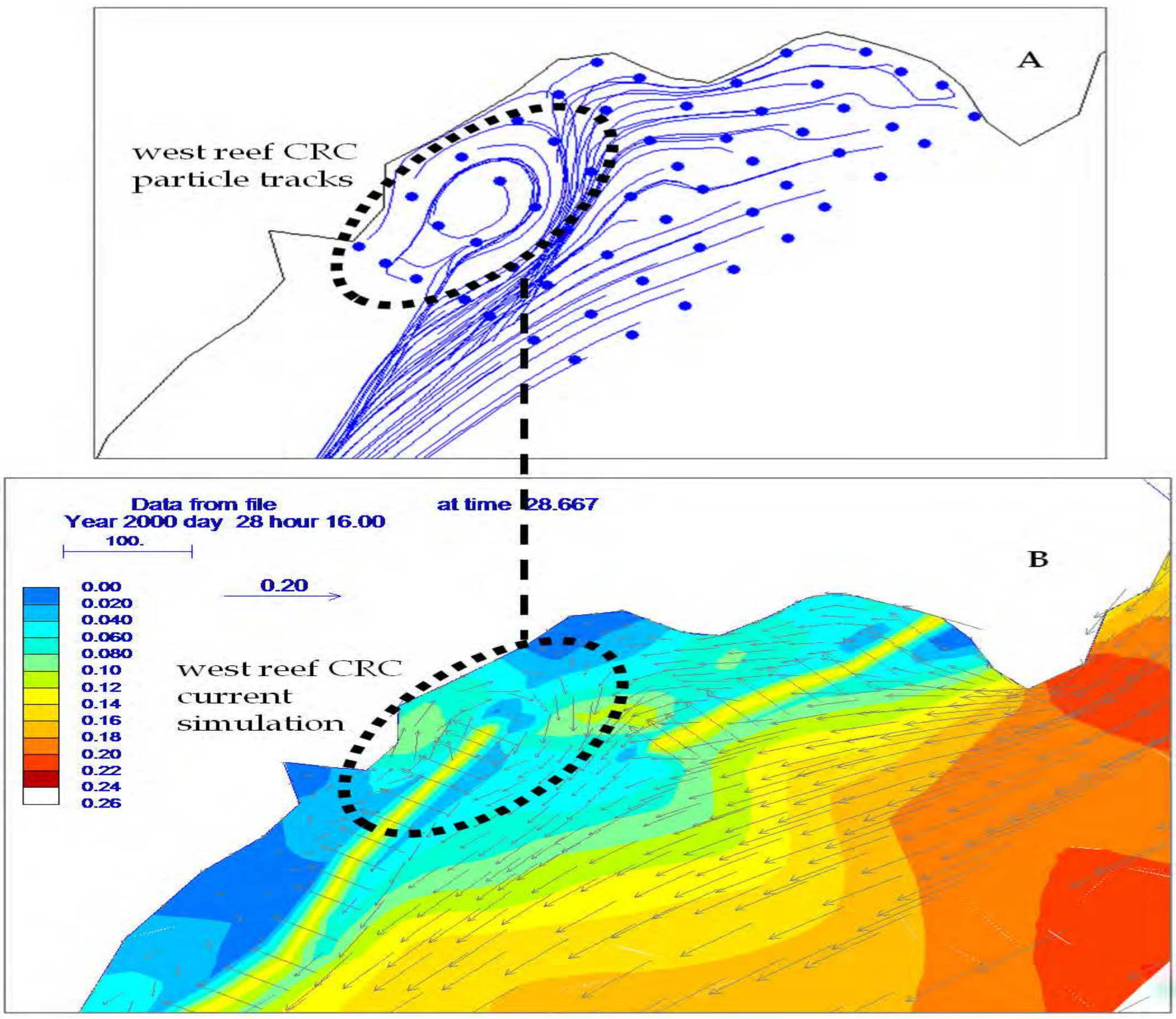

Fig. 11. Dominant west reef CRC in Wreck Bay is shown here typically occurring during neap periods when bay extension was due primarily to wind and over-the-reef forcing. CRC is displayed as circled area in model particle tracks (A) and model vectors (B). CRC formation on the opposing reef arm is weakened during dominance of the other.

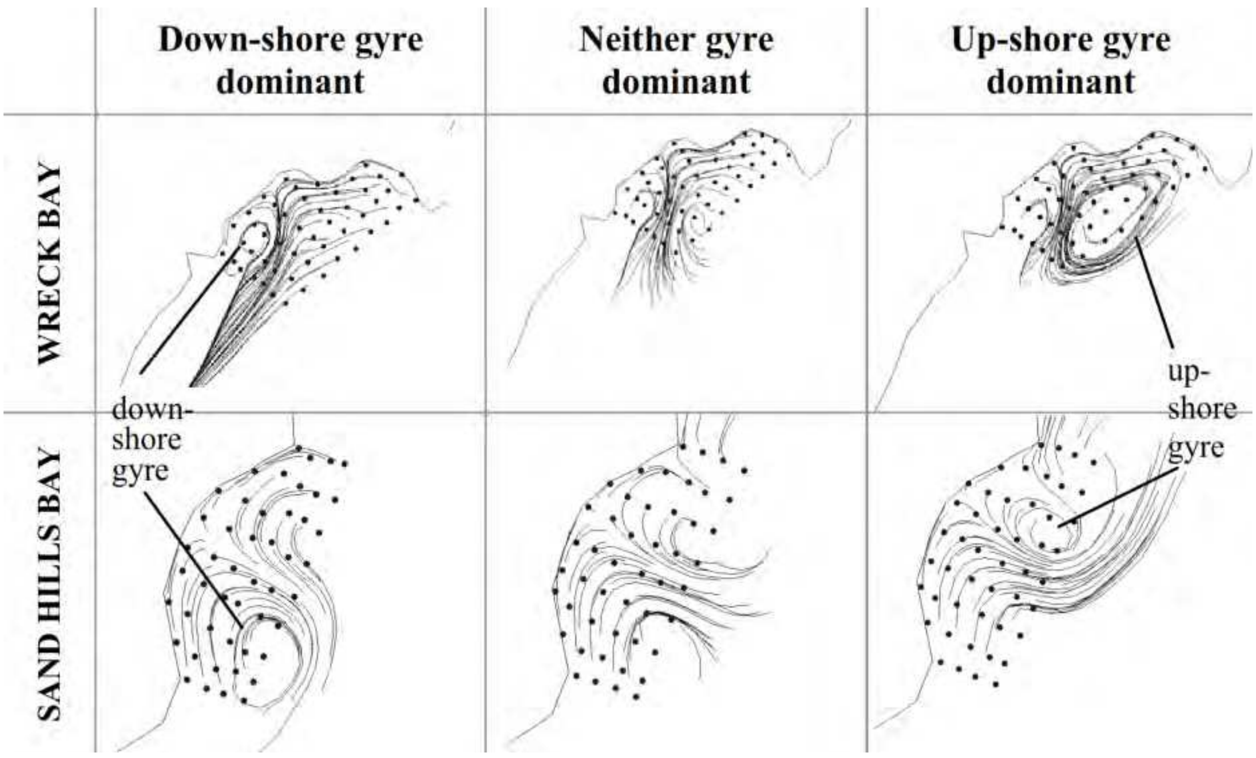

Fig. 12. RMTRK Tracking model outputs depicting gyre dominance cycling in Wreck Bay and Sand Hills Bay. Closed gyre formation is dominant on the down-shore reef during rising tide regimes, abate at high tide, then re-form on the up-shore reef during falling tide. The larger reef in both bays produced the larger dominant gyre resulting in the greater seaward extensions of the bay. The east reef for Wreck Bay and the south reef at Sand Hills Bay therefore expanded the bays the most.

6.3 Reef CRC persistence between paired reef arms

Persistence of one reef CRC over another was observed with the reef pairs and was characteristic of one reef only, unlike reef dominance that alternated between reefs. Persistence of a reef arm CRC occurred when, during conditions that caused the least change in current flow, the CRC was continuously propagated on that reef. This was observed during a combination of decreased over-the-reef flow and small changes in tidal amplitude, when the Wreck Bay west reef arm and the Sand Hills Bay south reef arm displayed continuous CRC while the other reef arms in the pair showed none, even during changing tidal cycles. This persistence, along with the larger west reef flow, has led to the west reef contributing more than the east reef overall to the channel flow in Wreck Bay.

6.4 Variability in retention

Sand Hills Bay retained particles longer than Wreck Bay in model simulations, with retention controlled mostly by the dominant reef gyre. The dominant reef gyre is maintained in Sand Hills Bay during the rising tide, while that of Wreck Bay is well-formed during the falling tide. This presents the likelihood that waterbourne particles flushed out of

Kingston Harbour to the north during a flood event undergo retention along the Hellshire shoreline all through the tidal cycle, particularly during wind clams, but alternating in these reefal bays depending on the stage of the cycle prevailing. The longest retention time derived from field data was 9 hrs (Maxam & Webber, 2010) and compares well with model results that showed the longer retention of particles ranging from 6 to 9 hrs.

Simulations also show that CRC presence is characterized by increased fluctuations in the retention of particles. Model simulations depicted that after 6 hrs, Wreck Bay and Sand Hills Bay showed the greatest variation in number of particles remaining and Engine Head Bay the least variation across all conditions. Therefore, those conditions that facilitated greater particle retention in the reefal bays, particularly wind calms (Maxam & Webber, 2010), significantly increased retention times over that of the open Engine Head Bay. The same is true for those conditions that facilitated decreased particle retention in the reefal bays where these were significantly lower than in the non-reefal bay.

Provided wind conditions did not dominate, Engine Head Bay produced similar retention times as particles oscillated back and forth inside the bay arc with the change of the tidal regime. This oscillation, however, did not extend outside the bay arc, unlike with the reefal bays. Reefal bays therefore display the ability to not only trap particles throughout tidal cycles, but also create a wider trapping area (extended seawards) than open bays along the Hellshire shoreline.

CRC strengthening was therefore evident

i. with the closure of the looping circulation;
ii. in the increased recirculation rate of particles resulting from increased gyre current speeds; and
iii. in the broad spatial extent of the CRC occupying a greater portion of the bay area.

Hence, the CRC is considered persistent because it continuously loops the reef, and is strengthened when gyres are closed and it broadens horizontally. This closing re-circulation demonstrates very well the connectivity and continuity of the channel outflow re-entering the bay over the reef, and therefore best confirms the reef as the circulatory centre of the bay. Model simulations did not produce a reversal in back-reef currents at any time, evidence that the CRC is never completely reversed but instead may become severely weakened, usually coinciding with very rare events of channel reversal at depth (recorded by field instruments in Maxam & Webber, 2010). The functional bay is therefore seen to exist around the reef such that the reef parabola are the center of the system. Increased flow over the reef, especially during the sea-breeze regime, caused surges in channel currents that would increase the speed of the current loop and result in faster flushing times. Reefal bay flushing and retention regimes have direct implications on the dynamics of vulnerable planktonic species important to reef establishment (Wolanksi & Sarsenski, 1997), and the ability of these bays to draw in, retain and flush pollutants (Black et al., 1990; Lasker & Kapela, 1997).

6.5 Bathymetric characteristics necessary for promoting CRC

The topography of the reefal bay allows it to produce signature dynamics driven primarily by over-the-reef flow, wind and tidal forcings. Waves break over the reef and the generated flow feed reef-parallel currents that in turn supply a major channel outflow. The channel (Figure 13) features significantly in this system and its prominence is the main bathymetric difference from other more popularly studied reef systems such as atolls, platform and ribbon reef. The channel in the reefal bay is the main conduit of back-reef water exiting to the sea, and therefore sets up the hydrodynamics to produce jet currents that help complete the circum-reef current. This CRC has been shown to either close in on itself , which is when gyres are formed that cause particles to re-circulate on the reef, or to flow along the fore-reef and join the general long-shore flow, causing particles to leave the system.

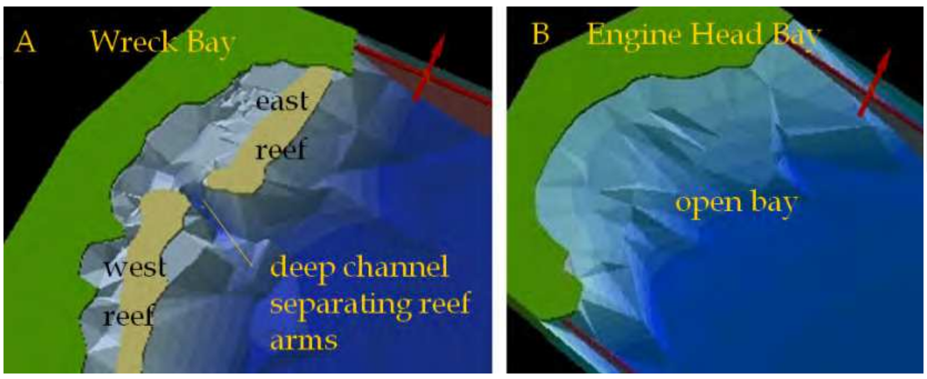

Fig. 13. Spatial 3D model of Wreck Bay (A) and Engine Head Bay (B) revealing their differences in topography. In Wreck Bay, reef arms are emergent at high tide and the deepest part of the system is its prominent channel. This is topographically more complex than the open, non-reefal Engine Head Bay (spatial 3D Models are exaggerated vertically).

Bathymetric characterization includes the reef arms, where their presence localizes the CRC and relative size becomes an important factor. The larger reef arm generates the more expansive gyres and therefore greatest emanations of the bay. This geomorphology is typical of many Caribbean reefal bays. By over-generalization, however, bays have been classified geomorphologically by variations in their coastlines' indented shape (Rea & Komar, 1975; Silvester et al., 1980). This has been applied to systems for which the circulation can be persistent or temporary. Gently-sloping shorelines, for example, exposed to wave action may contain gyre circulations, similar to the CRC, that comprise a seaward rip current diffusing beyond the breaker zone and returning landward as slow mass drift under wave action (Carter 1988). Unlike the reefal-bay system, however, the stability of these gyres is heavily dependent on high energy wave action and so rip features are hardly permanent or in the same location. Ultimately, the bathymetry unique to these reefal-bay systems is principal in forming and maintaining the CRC, as seen in the simulation of the longer-lasting gyres when both the wind and tidal contributions are reduced.

6.6 Reliability of the hydrodynamic model

The hydrodynamic model used flow over-the-reef along a boundary line to simulate wave breaking and captured the effects of shorter period wind-wave driven flow important in driving channel currents. Current simulations in the channel were therefore in good agreement with S4 field data and are considered most important in these models since they form the main link in the CRC formation, in addition to being the direct driver of CRC emanation and contraction. Simulations, however, fell short in capturing some effects caused by the reef flat (Cetina-Heredia et al., 2008), and the contribution of longer period swell, seiching and infra-gravity waves (Lugo-Fernandez et al., 1998; Pequignet, 2008). This affected the back-reef outputs where currents were faster and less variable than simulated by the RMA model. Results from the model, however, were sufficient for simulating the bay circulation around the reef, revealing signature patterns, and deriving the contributions of wind and tide regimes to driving gyre emanations.

7. Conclusion

The hydrodynamic modelling and tracking simulations were able to reproduce field observations, allowing the following signatures to be developed for characterizing the reefal bay system:

- A characteristic bathymetry comprised of reef arms broken by prominent channel, giving rise to a persistent circulation;
- A reef-centered circulation driven by wind, tides and over-the-reef flow;
- A reef-centered circulation that continuously looped the reef (circum-reef circulation or CRC) to form either a closed gyre (closed CRC) or to flow along the fore-reef as open loop (open CRC);
- A CRC that was persistent because it is always present and localized;
- A CRC with a spatial pulse indicated by cycles of expansion and contraction;
- The dominance of the CRC alternating between reef arms and dictating which reef arm was primarily responsible for bay extension;
- The persistence of particularly one reef arm's CRC regardless of the wind or tidal regime.

These signatures are now identified with the reefal bay system, where the reef is shown to be central to inducing the circum-reef circulation or CRC that encourages re-circulation of inner bay waters, and that this CRC formation is not found in non-reefal bays, where there is an absence of emergent reef between headlands. Driving forces such as wind, over-the-reef flow and tidal changes were responsible for maintaining the CRC including its contractions and emanations. These findings are important in their implications for stabilizing and protecting these systems as well as the shoreline of which they are a part. Incorporating the reef-parabola geomorphology as the centre of circulation gives predictability to other bay features such as the physicochemical, geo-physical and biological dynamics, which are all affected in greater part by local circulation. Many of these bays, for example, function as nurseries for marine and terrestrial species where their planktonic stages are directly influenced by current patterns and regimes. Identifying the CRC will aid in locating and protecting habitats conducive to plankton viability and survival, including reef growth and expansion.

8. Summary

Research on reefal bays revealed that inner bay waters exiting the channel between reefs re-circulated into the back-reef, and that this circulation was localized and permanent around reefs as the signature circulation. The distinctive topology of reef arms subtending the headland and separated by a prominent channel induced particles to circulate the reef in expanding and contracting gyres. Gyres expanded by as much as 98% of the horizontal distribution, with expansion and contraction linked to cyclical wind and tidal regimes, giving the reefal system a signature pulse in circulation. Strengthening of the circulation around the reef resulted in closure of looping circulation, increased recirculation rate of particles, increased gyre current speeds and broadening of the circulation's spatial extent.

One reef arm's circulation would dominate over the other at the peaks of these cycles, exhibiting gyre dominance. Increased variability of particle retention was also characteristic. These signatures were not evident in an adjacent open, non-reefal bay used as a comparison. The stability, spatial spread and localization of the circulation therefore defined this circum-reef circulation and identifies its association with reefal bays in particular, where the reef functions as the centre of a dynamic bay.

9. Acknowledgements

The authors are grateful to the Port Royal Marine Lab, the Center for Marine Sciences, the Japan International Corporation Agency and the Mona Geoinformatics Institute for providing funding, technical support and equipment to carry out this study. The Environmental Foundation of Jamaica in partnership with the Life Sciences Department, University of the West Indies, was significant in providing funding for training in hydrodynamic modelling. We acknowledge Christopher Burgess for guidance in the oceanographic statistics and modelling. Acknowledgement also goes to the dedication of Sean Townsend and the many student volunteers from the Department of Life Sciences, University of the West Indies, in assisting with the field work.

10. References

Black, K.P.; Gay, S.L. & Andrews, J.C. (1990). Residence times of neutrally-buoyant matter such as larvae, sewage or nutrients on coral reefs. *Coral Reefs* 9: 105-114.

Burgess, P.; Irwin, M.; Maxam, A. & Townsend, S. (2005). Oceanographic Study of Sand Hills Bay. Civil Environmental and Coastal Solutions Engineer's Report to the UDC, 79 pp, Kingston Jamaica.

Carter, R.W.G. (1988). Coastal Environments: an introduction to the physical, ecological and cultural systems of coastlines. Academic Press. Great Britain.

Cetina-Heredia, P.; Connolly, S. & Herzfeld, M. (2008). Modeling larval retention around reefs by local scale circulation features, *Proceedings of the 11th International Coral Reef Symposium*, July, 2008, Florida.

Douillet, P.; Ouillon, S. & Cordier, E. (2001). A numerical model for fine suspended sediment transport in the southwest lagoon of New Caledonia. *Coral Reefs* 20: 361-372.

Feddersen, F. & Trowbridge, J. H. (2005). The effect of wave breaking on surf-zone turbulence and alongshore currents: A modelling study. *Journal of Physical Oceanography*. 35: 2187 – 2203.

Foreman, M.G.G. (1977). Manual for Tidal Heights Analysis and Prediction. *Pacific Marine Science Report* 77-10, Institute of Ocean Sciences, Patricia Bay, Sidney, B.C., 58 pp.

Goodbody, I.; Bacon, P.; Greenaway, A.; Head, S.; Hendry, M. & Jupp, B. (1989). Caribbean Coastal Management Study: The Hellshire Coast, St. Catherine, Jamaica. *Marine Science Unit Research Report* no.1. Ed. I. Goodbody. University of the West Indies. pp 176.

Gourlay, M.R. & Colleter, G. (2005). Wave-generated flow on coral reef – an analysis for two-dimensional horizontal reef-tops with steep faces. *Coastal Engineering*. 52: 353 – 387.

Gunaratna, P.P.; Justesen, P. & Abeysirigunawardena, D.S. (1997). Mathematical modeling of hydrodynamics in a reef protected coastal stretch. 2nd DHI Software User Conference, Denmark. Paper C7-1.

Hasselmann, K.; Barnett, T. P.; Bouws, E.; Carlson, H.; Cart-wright, D. E.; Enke, K.; Ewing, J. A.; Gienapp, H.; Hasselmann, D. E.; Kruseman, P.; Meerburg, A.; Muller, P.; Olbers, D. J.; Richter, K.; Sell, W. & Walden, H. (1973). Measurements of wind-wave growth and swell decay during the Joint North Sea Wave Project (JONSWAP), Erganzungsheft zur Deutschen Hydrographischen Zeitschrift, Reihe A. 12. 95 pp, Deutsches Hydrographisches Institut, Hamburg, Germany.

Hearn, C. J. (1999). Wave-breaking hydrodynamics within coral reef systems and the effect of changing relative sea level. *Journal of Geophysical Research*, Series C 104, 30007 – 30019.

Hearn, C.J. (2001). Introduction to the special issue of *Coral Reefs* on "Coral Reef Hydrodynamics". *Coral Reefs* 20: 327-329.

Hendry, M.D. (1983). The influence of the sea-land breeze regime on beach erosion and accretion : an example from Jamaica. *Caribbean Geography, 1* (1), 13-23.

King, I.P. (2003). A finite element model for stratified flow; RMA-10 version 7.1B. 66 pp, Resource Modelling Associates, Sydney, Australia.

King, I.P. (2005). A particle tracking model compatible with the RMA series of finite element surface water models; RMATRK version 3.2, 19 pp, Resource Modelling Associates, Sydney, Australia.

Kirby, J.T. & Dalrymple, R.A. (1991). User's Manual -Combined Refraction/Diffraction Model: REF/DIF 1 Version 2.3. Center for Applied Coastal Research. University of Delaware. Newark, Delaware.

Kraines, S.B.; Yanagi, T.; Isobe, M. & Komiyama, H. (1998). Wind-wave driven circulation on the coral reef at Bora Bay, Miyako Island. *Coral Reefs*. 17: 133-143.

Lasker, H.R. & Kapela, W.J. Jr. (1997). Heterogeneous water flow and its effects on the mixing and transport of gametes. *Proceedings of the 8th International Coral Reef Symposium*. 2: 1109-1114.

Lugo-Fernandez, A.; Roberts, H.H. & Wiseman, W.J. (1998). Water level and currents of tidal and infragravity periods at Tague Reef, St. Croix (USVI). *Coral Reefs*, 17 (4), 343-349.

Maxam, A.M. & Webber, D.F. (2009). Using the distribution of physicochemical variables to portray reefal bay waters. *Journal of Coastal Research*, 25 (6), 1210-1221.

Maxam, A.M. & Webber, D.F. (2010). The influence of wind-driven currents on the circulation and bay dynamics of a semi-enclosed reefal bay, Jamaica. *Estuarine, Coastal and Shelf Science*, 87, 535-544.

Mellor, G.L. & Yamada, T. (1982). Development of a Turbulence Closure Model for Geophysical Fluid Problems. *Reviews of Geophysics and Space Physics*, 20 (4), pp 851-875.

Nwogu, O.; Demirbilek, Z. & Merrifield, M. (2008). Non-linear wave transformation over shallow fringing reefs, *Proceedings of the 11th International Coral Reef Symposium*, July, 2008. Florida.

Nybakken, J.W. (1997). Marine Biology: An Ecological Approach, 4th ed. Addison-Wesley Educational Publishers Inc.

Pequignet, A. (2008). Importance of infragravity band in the wave energy budget of a fringing reef, *Proceedings of the 11th International Coral Reef Symposium*, July, 2008. Florida.

Prager, E.J. (1991). Numerical simulation of circulation in a Caribbean-type back reef lagoon, *Coral Reefs*, 10, 177-182.

Rea, C.C. & Komar, P.D. (1975). Computer simulation models of a hooked beach's shoreline configuration. *Journal of Sedimentology and Petrology* 45: 866-872.

Roberts, H.H. (1980). Physical processes and sediment flux through reef-lagoon systems, *Proc 17th Int. Coastal Engineering Conf.* , ASCE, Sydney, Australia, pp 946-962.

Roberts, H.H. & Suhayda, J.N. (1983). Wave-current interactions on a shallow reef. *Coral Reefs*, 1, 209-214.

Roberts, H.H.; Lugo, A.; Carter, B. & Simms, M. (1988). Across reef flux and shallow subsurface hydrology in modern coral reefs, *Proceedings of the 6th International Coral Reef Symposium*, 2, 509-515. Townsville, Australia.

Roberts, H.H.; Wilson, P.A. & Lugo-Fernandez, A. (1992). Biologic and geologic responses to physical processes: examples from modern reef systems of the Caribbean-Atlantic region, *Continental Shelf Res*earch, 12 (7/8), 809-834.

Sammarco, P.W. & J.C. Andrews (1989). The Helix experiment: differential localised dispersal and recruitment patterns in Great Barrier Reef corals, *Limnolology and Oceanography,* 34, 898-914.

Silvester, R., Tsuchiya, Y., & Shibano, Y. (1980). Zeta bays, pocket beaches and headland control. *Proceedings in the 17th International Conference of Coastal Engineering*., ASCE 2: 1306-1319.

Smith, N.P. (1985). The decomposition and simulation of the longitudinal circulation in a coastal lagoon. *Estuarine Coastal Shelf Science* 21: 623-632.

Symonds, G.; Black, K.P. & Young, I.R. (1995). Wave driven flow over shallow reefs. *Journal of Geophysical Research* 100 (C2): 2639-2648.

Tartinville, B.; Deleersnijder, E. & Rancher, J. (1997). The water residence time in the Mururoa atoll lagoon: sensitivity analysis of a three-dimensional model. *Coral Reefs* 16: 193-203.

Van der Meer, J.W. (2002). Wave run-up and wave overtopping on dikes. (in Dutch; original title: Golfoploop en golfoverslag bij dijken). WL Delft Hydraulics, *Report H2458/H3051*, June 1997.

Webber, D.F. (1990). Phytoplankton populations of the coastal zone and nearshore waters of Hellshire: St. Catherine, Jamaica. Ph.D. Thesis, 285 pp, University of the West Indies, Mona.

White, M. (1982). Ground water lenses in Hellshire Hills (East), a minor source of water for Hellshire Bay. Hydrology Consultants Ltd., Kingston MS Report. 34 pp.

Wolanski, E. & Sarsenski, J. (1997). Larvae dispersion in coral reefs and mangroves. *American Science*. 85: 236-243.

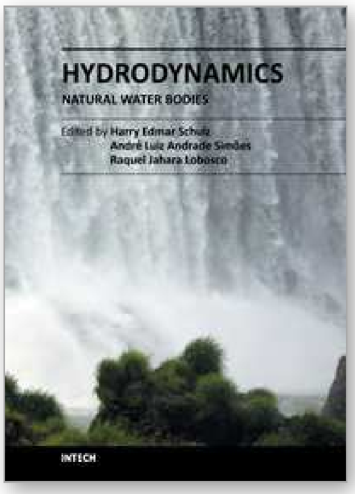

Hydrodynamics - Natural Water Bodies
Edited by Prof. Harry Schulz

ISBN 978-953-307-893-9
Hard cover, 286 pages
Publisher InTech
Published online 05, January, 2012
Published in print edition January, 2012

The knowledge of the characteristics of the fluids and their ability to transport substances and physical properties is relevant for us. However, the quantification of the movements of fluids is a complex task, and when considering natural flows, occurring in large scales (rivers, lakes, oceans), this complexity is evidenced. This book presents conclusions about different aspects of flows in natural water bodies, such as the evolution of plumes, the transport of sediments, air-water mixtures, among others. It contains thirteen chapters, organized in four sections: Tidal and Wave Dynamics: Rivers, Lakes and Reservoirs, Tidal and Wave Dynamics: Seas and Oceans, Tidal and Wave Dynamics: Estuaries and Bays, and Multiphase Phenomena: Air-Water Flows and Sediments. The chapters present conceptual arguments, experimental and numerical results, showing practical applications of the methods and tools of Hydrodynamics.

InTech Europe
University Campus STeP Ri
Slavka Krautzeka 83/A
51000 Rijeka, Croatia
Phone: +385 (51) 770 447
Fax: +385 (51) 686 166
www.intechopen.com

InTech China
Unit 405, Office Block, Hotel Equatorial Shanghai
No.65, Yan An Road (West), Shanghai, 200040, China
中国上海市延安西路65号上海国际贵都大饭店办公楼405单元
Phone: +86-21-62489820
Fax: +86-21-62489821